2124–2136 *Nucleic Acids Research, 2017, Vol. 45, No. 4* *Published online 2 December 2016*
doi: 10.1093/nar/gkw1120

Identification of 2-methylthio cyclic *N*^{6}-threonylcarbamoyladenosine (ms^{2}ct^{6}A) as a novel RNA modification at position 37 of tRNAs

Byeong-il Kang[1,†], Kenjyo Miyauchi[1,†], Michal Matuszewski[2], Gabriel Silveira D'Almeida[3], Mary Anne T. Rubio[3], Juan D. Alfonzo[3], Kazuki Inoue[1], Yuriko Sakaguchi[1], Takeo Suzuki[1], Elzbieta Sochacka[2,*] and Tsutomu Suzuki[1,*]

[1]Department of Chemistry and Biotechnology, Graduate School of Engineering, University of Tokyo, Tokyo 113-8656, Japan, [2]Institute of Organic Chemistry, Faculty of Chemistry, Lodz University of Technology, Lodz 90-924, Poland and [3]Department of Microbiology and The Center for RNA Biology, The Ohio State University, Columbus, OH 43210, USA

Received October 11, 2016; Editorial Decision October 26, 2016; Accepted November 09, 2016

ABSTRACT

Transfer RNA modifications play pivotal roles in protein synthesis. *N*^{6}-threonylcarbamoyladenosine (t^{6}A) and its derivatives are modifications found at position 37, 3′-adjacent to the anticodon, in tRNAs responsible for ANN codons. These modifications are universally conserved in all domains of life. t^{6}A and its derivatives have pleiotropic functions in protein synthesis including aminoacylation, decoding and translocation. We previously discovered a cyclic form of t^{6}A (ct^{6}A) as a chemically labile derivative of t^{6}A in tRNAs from bacteria, fungi, plants and protists. Here, we report 2-methylthio cyclic t^{6}A (ms^{2}ct^{6}A), a novel derivative of ct^{6}A found in tRNAs from *Bacillus subtilis*, plants and *Trypanosoma brucei*. In *B. subtilis* and *T. brucei*, ms^{2}ct^{6}A disappeared and remained to be ms^{2}t^{6}A and ct^{6}A by depletion of *tcdA* and *mtaB* homologs, respectively, demonstrating that TcdA and MtaB are responsible for biogenesis of ms^{2}ct^{6}A.

INTRODUCTION

RNA modifications are a type of qualitative information embedded in RNA molecules (1). To date, about 140 species of modified nucleosides have been identified in various RNAs from all domains of life (2). tRNAs contain a number of chemical modifications that are required for accurate translation of the genetic code and stabilization of the tRNA tertiary structure (3–5). In particular, a wide variety of modifications is present in the anticodon loop, especially at the first position of the anticodon (position 34) and position 37, which is 3′-adjacent to the anticodon. These modifications play critical roles in modulating codon recognition and ensuring accurate translation (6).

N^6-threonylcarbamoyladenosine (t^{6}A) (Supplementary Figure S1) and its derivatives are evolutionarily conserved essential modified bases at position 37 of tRNAs responsible for recognition of adenosine-starting codons (ANN codons) (7). The bulky side chain of t^{6}A stabilizes the anticodon loop, promoting accurate decoding of ANN codons during protein synthesis (8,9). In addition, t^{6}A is required for efficient aminoacylation of tRNA and efficient translocation, and it also prevents leaky scanning of initiation codons and read-through of stop codons. The biogenesis of t^{6}A has been studied extensively. In *E. coli*, four enzymes, TsaC (YrdC), TsaD (YgjD), TsaB (YeaZ), and TsaE (YjeE), are required to synthesize t^{6}A; L-threonine, adenosine triphosphate (ATP) and bicarbonate as substrates (8). In yeast, the YrdC homolog Sua5 and several components of the EKC-KEOPS complex, including Kae1, Pcc1, Gon7 and Bud32, are involved in t^{6}A formation (10–12).

The presence of t^{6}A in tRNAs from *E. coli* and yeast was first documented more than four decades ago (13). In 2013, however, we showed that most fraction of t^{6}A in *E. coli* tRNAs is a hydrolyzed artifact of cyclic t^{6}A (ct^{6}A) (Supplementary Figure S1) (9). ct^{6}A is an additional modification of t^{6}A that enhances tRNA decoding activity. ct^{6}A is present in tRNAs from certain groups of bacteria, fungi, plants and some protists, but not in tRNAs of mammals, archaea or other bacteria. In *E. coli*, little t^{6}A is present in tRNAs because almost all t^{6}A is converted to ct^{6}A via an ATP-dependent dehydration catalyzed by TcdA. We also identified two additional factors, CsdA and CsdE, which are required for efficient ct^{6}A formation. CsdA is a cysteine

*To whom correspondence should be addressed. Tel: +81 3 5841 8752; Fax: +81 3 5841 0550; Email: ts@chembio.t.u-tokyo.ac.jp
Correspondence may also be addressed to Elzbieta Sochacka. Tel: +48 42 631 31 55; Fax: +48 42 636 55 30; Email: elzbieta.sochacka@p.lodz.pl
†These authors contributed equally to this work as the first authors.

desulfurase, and CsdE is a sulfur acceptor protein, implying that sulfur relay is involved in efficient formation of ct^6A.

Initially, mass spectrometric and nuclear magnetic resonance (NMR) analyses determined the chemical structure of ct^6A to be a cyclized active ester of the oxazolone ring (Supplementary Figure S1) (9,14). Very recently, however, X-ray crystallography of synthetic ct^6A nucleoside revealed the existence of a distinct isoform with a hydantoin structure (Supplementary Figure S1) (15). LC/MS co-injection analyses showed that chemically synthesized ct^6A nucleoside and natural ct^6A in *Escherichia coli* tRNAs co-elute as a single peak by both reverse-phase and hydrophilic interaction liquid chromatography. They also exhibit identical patterns of product ions in collision-induced dissociation (CID) and a characteristic UV spectrum with maximum absorption at 269 nm. These observations strongly suggest that the hydantoin isoform of ct^6A is actually present in *E. coli* tRNAs.

Another derivative of t^6A, N^6-methyl-N^6-threonylcarbamoyladenosine (m^6t^6A) (Supplementary Figure S1), is present in tRNAs from bacteria, fly, plants and mammals. In *E. coli*, m^6t^6A is present at position 37 of two species of $tRNA^{Thr}$ responsible for translating ACY codons. We identified TrmO, a member of a novel class of AdoMet-dependent RNA methyltransferase, as the enzyme responsible for N^6 methylation of m^6t^6A37 of bacterial $tRNA^{Thr}$ (16). Its human homolog, TRMO, is responsible for formation of m^6t^6A37 in cytoplasmic $tRNA^{Ser}$. Lack of TrmO decreases attenuation activity of the *thr* operon, indicating that N^6 methylation of m^6t^6A37 ensures efficient decoding of ACY.

2-Methylthio-N^6-threonylcarbamoyladenosine (ms^2t^6A) (Figure 1A) is another derivative of t^6A found in $tRNA^{Lys}$ from *Bacillus subtilis* (Figure 1B), *Trypanosoma* (Figure 1B), plants and mammals (17–20). The methylthiolation of ms^2t^6A is required for the accurate decoding of Lys codons. *B. subtilis* MtaB (21,22) and human Cdkal1 (23) are the methylthiotransferases responsible for ms^2t^6A formation in tRNAs. Mutations in *CDKAL1* are associated with risk of type 2 diabetes (24); consistent with this, pancreatic β-cell–specific knockout of mouse *Cdkal1* results in a phenotype similar to that of type 2 diabetes (23). The presence of ct^6A and TcdA homologs in *B. subtilis*, plants and *Trypanosoma* prompted us to speculate that the cyclic form of ms^2t^6A (ms^2ct^6A) (Figure 1A) would also be present in these organisms. As with ct^6A, ms^2ct^6A must be hydrolyzed and converted to ms^2t^6A during tRNA preparation or conventional nucleoside analysis, which explains why it has not been previously detected. Indeed, a Tris-adduct of ms^2t^6A was detected in $tRNA^{Lys}$ (Figure 1B) from *Trypanosoma brucei* (19), indicating the presence of ms^2ct^6A; primary amines easily react with ct^6A to form amine adducts of t^6A (25).

Here, we describe ms^2ct^6A as a novel derivative of ct^6A in tRNAs from *B. subtilis*, plants, and *T. brucei*. The chemical structure of ms^2ct^6A in natural tRNA was confirmed by LC/MS co-injection with the chemically synthesized authentic nucleoside. We also confirmed that orthologs of TcdA and MtaB are responsible for biogenesis of ms^2ct^6A in *B. subtilis* and *T. brucei*. In addition, we observed slower growth of *T. brucei* when the TcdA ortholog was down-regulated in the presence of cycloheximide, indicating that cyclic form of t^6A is involved in integrity of protein synthesis.

MATERIALS AND METHODS

Bacterial strains and cultivation

B. subtilis str. 168 (WT) was kindly provided by Akiko Soma (Chiba University). *B. subtilis* strains were grown overnight in LB medium at 37°C. The Δ*yqeV* strain harboring the erythromycin resistance marker (Em^r) was obtained from the National BioResource Project (National Institute of Genetics, Japan). The Δ*yrvM* strain was constructed from the WT strain, and the Δ*yqeV*/Δ*yrvM* double-deletion strain was constructed from the Δ*yqeV* strain by homologous recombination (26,27). The 5′ upstream and 3′ downstream regions (700–800 nt) of the *yrvM* gene were PCR-amplified from *B. subtilis* str. 168 genomic DNA with pairs of primers, 5′-ggcacctattctgtatccattgatg-3′ and 5′-aagcgcagctcttgatgatcaaggctgttttttttg-3′ and 5′-tgaggatgaaggctgatccatgagcagccg-3′ and 5′-gagcatgatccggaagaaggc -3′, respectively. Chloramphenicol resistant gene (Cm^r) gene was PCR-amplified from pCBB31 (28) using a set of primers, 5′-gatcatcaagagctgcgctttttttgtgtc-3′ and 5′-tggatcagccttcatcctcatattataaaagccag-3′. These 3 products were ligated by PCR using primers, 5′-ggcacctattctgtatccattgatg-3′ and 5′-gagcatgatccggaagaaggc-3′, and subjected to the nested PCR amplification using a pair of primers, 5′-tccatgatgatcaggcgatgga-3′ and 5′-ggaagaaggccgtttttacgca-3′. The resultant PCR fragment was used for transformation.

Total RNA extraction

B. subtilis cells were suspended with 5 ml of RNA extraction buffer [50 mM NaOAc (pH 5.2) and 10 mM $Mg(OAc)_2$ (pH 5.2)] and vigorously stirred for 10 min at room temperature. Next, 5 ml of water-saturated phenol was added and stirred for 10 min at room temperature. The mixture was frozen with liquid nitrogen and thawed in water; this process was repeated twice. The thawed solution was stirred for 50 min at room temperature. The aqueous phase was separated by centrifugation and washed once with chloroform, followed by re-extraction with 0.75 volumes of Trizol-LS (Life Technologies). Then, total RNA was precipitated with 2-propanol. The RNA pellet was dissolved in deionized water and subjected to ethanol precipitation; the resultant pellet was rinsed with 80% ethanol and dried. Thus, prepared RNA can be stored in pellet form for a long period of time without hydrolysis of ct^6A and ms^2ct^6A. For use in all experiments, pellets were dissolved in ultrapure water.

Total RNA of spinach and *Arabidopsis thaliana* were extracted from plants as previously described (9). *Nicotiana tabacum* total RNA was obtained by the same procedure from tobacco BY-2 cells cultured for 1 week in modified Linsmaier and Skoog medium (29). Total RNA samples of spinach and tobacco were subjected to brief purification by weak anion exchange chromatography with DEAE Sepharose Fast Flow (GE Healthcare) to remove bulk contaminants and rRNA, as described (30).

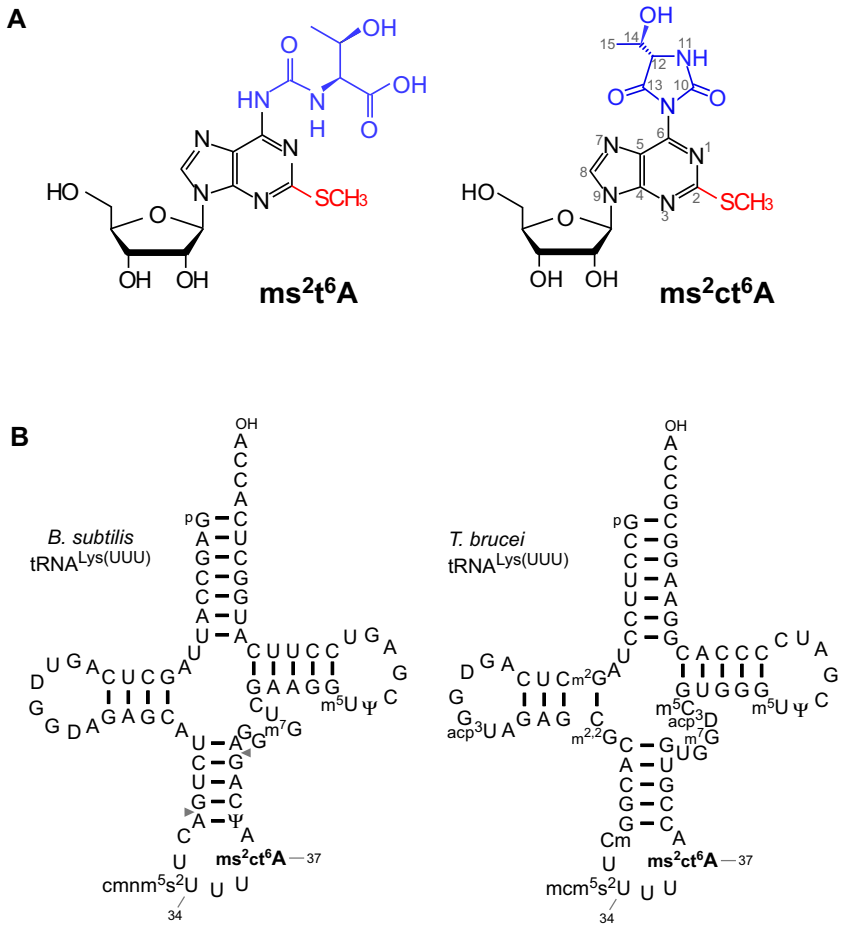

Figure 1. Detection of 2-methylthio-cyclic-N^6-threonylcarbamoyladenosine (ms^2ct^6A). (**A**) The chemical structure of ms^2t^6A (left) and ms^2ct^6A (right). The 2-methylthio modification is shown in red, and the N^6-threonylcarbamoyl group and its hydantoin form are shown in blue. (**B**) Secondary structures of *B. subtilis* $tRNA^{Lys}$ (left) and *T. brucei* $tRNA^{Lys}$ (right) with post-transcriptional modifications: dihydrouridine (D), 5-carboxymethylaminomethyl-2-thiouridine ($cmnm^5s^2U$), 2-methylthio cyclic N^6-threonylcarbamoyladenosine (ms^2ct^6A), pseudouridine (Ψ), 7-methylguanosine (m^7G), 5-methyluridine (m^5U), N^2-methylguanosine (m^2G), 3-(3-amino-3-carboxypropyl)uridine (acp^3U), N^2, N^2-dimethylguanosine ($m^{2,2}G$), 2′-*O*-methylcytidine (Cm), 5-methoxycarbonylmethyl-2-thiouridine (mcm^5s^2U), 3-(3-amino-3-carboxypropyl)dihydrouridine (acp^3D), 5-methylcytidine (m^5C). The position numbers of the residues are displayed according to the nucleotide numbering system (44). Pairs of gray triangles in *B. subtilis* $tRNA^{Lys}$ indicate the positions of cleavage by RNase T_1 that generate RNA fragments containing the anticodon region.

Isolation of *B. subtilis* $tRNA^{Lys}$

B. subtilis $tRNA^{Lys}$ was isolated from *B. subtilis* total RNA by reciprocal circulating chromatography, as described previously (9,31). The DNA probe, TGGTGAGCCATGAAGGACTCGAACCTTCGA with 5′-terminal EC amino linker was covalently immobilized on NHS-activated Sepharose 4 Fast Flow (GE Healthcare). Fifty one micrograms of highly purified $tRNA^{Lys}$ was obtained from 1.7 mg total RNA.

Nucleoside preparation

Before digestion, total RNA was pre-cleared by gel filtration on a Centri-Sep spin column (Princeton Separations) with deionized water or trimethylamine (TMA)-HCl (pH 7.0) buffer to remove contaminants that could interfere with the ionization efficiency of nucleosides. For this experiment, enzymes including nuclease P1 (Wako Pure Chemical Industries), phosphodiesterase I (PDase I, Worthington Biochemical Corporation) and bacterial alkaline phosphatase (BAP from *E. coli* C75, Wako Pure Chemical Industries) were dialyzed with deionized water and stored at −30°C until use. Phosphodiesterase II (PDase II, from bovine spleen, Sigma) was dissolved in 10 mM TMA-AcOH (pH 5.3) buffer and centrifuged. The supernatant was filtered through a 0.22 μm Ultrafree-MC unit (Merck-Millipore) and stored at −30°C.

For conventional digestion (32), 40 μg of total RNA was digested at 37°C for 1 h in a 25–50 μl reaction mixture consisting of 0.1 U nuclease P1 and 25 mM NH_4OAc (pH 5.3), followed by addition of 0.1 volume of 1 M ammonium bicarbonate (pH 8.2) and 0.08 U BAP, and then incubated at 37°C for 3 h.

For neutral digestion (9), 40 μg of total RNA was digested at 37°C for 1 h in a 25–50 μl reaction mixture consisting of 0.1 U nuclease P1 and 25 mM NH_4OAc (pH 5.3), followed by addition of 0.1 volume of TMA-HCl (pH 7.0) and 0.127 U PDase I, and then incubated at 37°C for 1 h.

The prepared nucleotides were dephosphorylated with 0.08 U BAP at 37°C for 3 h at neutral pH.

Digestion of plant and several other RNAs was carried out by one-step acidic digestion. Specifically, a solution (typically 40 μl) containing 1 μg/μl total RNA, 20 mM TMA acetate (pH 5.3), nuclease P1 (0.1 units for 40 μg of RNA), PDase II (0.1 units for 40 μg of RNA) and BAP (0.16 units for 40 μg of RNA) was incubated at 37°C for 1 h. In this procedure, PDase II was used for complete digestion of hypermodified adenosines under acidic conditions. We observed conversion of adenosine and N^6-methyladenosine (m^6A) to inosine, indicating contamination by adenosine deaminase activity in the Sigma PDase II product (P9041). t^6A derivatives remained intact under these conditions.

LC/MS analyses of total nucleosides and isolated tRNA

LC/MS analyses of total nucleosides were performed essentially as described previously (9,33–34), using an LCQ Advantage ion-trap (IT) mass spectrometer (Thermo Fisher Scientific) equipped with an ESI source and an HP1100 liquid chromatography system (Agilent Technologies) or a Q Exactive hybrid Quadrupole-Orbitrap mass spectrometer (Thermo Fisher Scientific) equipped with an ESI source and an Ultimate 3000 liquid chromatography system (Dionex).

For RPC/ESI-MS with an LCQ Advantage instrument, nucleosides were separated on an Inertsil ODS-3 column (2.1 mm × 250 mm, GL sciences) and analyzed as described previously (34). For RPC/ESI-MS with a Q Exactive instrument, digests were separated on a Sunshell C18 column (2.6 μm core-shell silica particle, 2.1 × 150 mm, ChromaNik Technologies). The mobile phase consisted of 5 mM ammonium acetate (pH 5.3) (solvent A) and acetonitrile (ACN) (solvent B). The gradient program was as follows: 0–40% B from 0 to 30 min, 40% B for 5 min and then 0% B at a flow rate of 75 μl/min. Nucleoside digest (8–12 μg) or synthetic ms^2ct^6A (100–500 pmol) dissolved in LC/MS grade ultrapure water (Wako) was injected.

For HILIC/ESI-MS, a ZIC-cHILIC column (3 μm particle size, 2.1 × 150 mm, Merck-Millipore) was used on a Q Exactive instrument (33). The mobile phase consisted of 5 mM ammonium acetate (pH 5.3) (solvent A) and ACN (solvent B). Total nucleosides (8–12 μg) or synthetic ms^2ct^6A (450–500 fmol) dissolved in 90% ACN was injected and chromatographed at a flow rate of 100 μl/min in a multi-step linear gradient: 90–40% B from 0 to 30 min, 40% B for 10 min and then 0% B. Proton adducts of nucleosides were scanned in a positive polarity mode over a range of m/z 110–700 or 110–900.

For RNA fragment analysis of isolated tRNA, *B. subtilis* $tRNA^{Lys}$ was digested by RNase T_1, followed by subjected to capillary liquid chromatography (LC) coupled to nano electrospray (ESI)/mass spectrometry (MS) on a linear ion trap-Orbitrap hybrid mass spectrometer (LTQ Orbitrap XL; Thermo Fisher Scientific) as described (9,34).

Chemical synthesis of ms^2ct^6A

The substrate nucleoside, 2-methylthio-N^6-threonylcarbamoyladenosine (ms^2t^6A) was synthesized according to the procedures described previously (35–38). Cyclization of ms^2t^6A to form ms^2ct^6A was performed on the basis of carbodiimide chemistry. ms^2t^6A (10 mg, 0.022 mmol) was dissolved in anhydrous DMF (1 ml) and mixed with EDC·HCl (42 mg, 0.22 mmol). The reaction mixture was stirred at room temperature. After 3 h, consumption of all substrate was confirmed by TLC analysis (*n*BuOH/H_2O, 85/15, v/v, R_f values of ms^2t^6A and ms^2ct^6A are 0.15 and 0.43, respectively). The solvent was removed under reduced pressure, and the crude product was purified by reverse-phase chromatography (Ascentis C18 HPLC Column, 10 μm, 21.2 × 250 mm) at a flow rate of 7 ml/min with a linear gradient of acetonitrile in 0.1% acetic acid (B) and water (A) as follows: 2–30% B from 0 to 40 min, 30–50% from 40 to 45 min, 50–2% B from 45 to 47 min, 2% B for 3 min. The ms^2ct^6A fraction (22.35 min) was collected and evaporated to dryness. Yield of ms^2ct^6A nucleoside was 44% (4.2 mg).

The purity of ms^2ct^6A was checked by high performance liquid chromatography (HPLC) analysis using an XTerra® Waters column (MS C8, 5 μm, 4.6 × 150 mm, 100 Å) (Supplementary Figure S2). The mobile phase consisted of 5 mM sodium acetate (pH 7) in water (solvent A) and ACN (solvent B). Chemically synthesized ms^2t^6A (A) and ms^2ct^6A (B) were chromatographed at a flow rate of 1 ml/min with a dual-step linear gradient: 0–20% B from 0 to 30 min, and 20–40% B from 30 to 40 min. Isolated ms^2ct^6A was characterized by UV spectroscopy (Supplementary Figure S3), IR spectroscopy (Supplementary Figure S4), ^{1}H-NMR (Supplementary Figure S5), ^{13}C-NMR (Supplementary Figure S6) and high resolution MS (Supplementary Figure S7).

Cultivation and RNAi of *T. brucei*

Partial segments of the coding sequences of the Tb427tmp.02.2830 (*TbTcdA*) and Tb427.06.3510 (*TbMtaB*) from *T. brucei* were cloned into the tetracycline-inducible RNAi vector p2T7-177. These plasmids were then linearized by *Not*I digestion and introduced into procyclic *T. brucei* 29-13 cells for genomic integration; clonal lines were obtained by limiting dilution. The cell lines were grown in SDM-79 medium, and RNAi was induced by addition of 1 μg/ml tetracycline. Cell counts were taken every 24 h using a Beckman Z2 Coulter counter over the course of 12 days post-induction in the presence or absence of tetracycline (1 μg/ml) and cycloheximide (50 μg/ml).

Total RNA was extracted from uniduced and RNAi-induced *T. brucei* cells using a standard protocol (39). The steady-state levels of individual mRNAs were measured by RT-PCR. The cDNAs of *TbMtaB* (677 bps) and *TbTcdA* (443 bps) were amplified using the following primers: 5′-attcacttaacttccctatttgc-3′ and 5′-gttctgacagcattcttcaaacc-3′ for *TbMtaB*, and 5′-gcctaccaaccgggaagccttcttg-3′ and 5′-ggattgcattgacagcgtcgagtgtaag-3′ for *TbTcdA*.

PCR products were then analyzed by agarose gel electrophoresis. The same reaction performed without reverse transcriptase was used as a negative control (RT-).

RESULTS

Identification of ms^{2}ct^{6}A in *B. subtilis* tRNAs

We previously detected ct^{6}A in total nucleosides of *B. subtilis* tRNAs digested under neutral conditions (9). Consistent with this finding, the *B. subtilis* YrvM is an ortholog gene of TcdA, which catalyzes ATP-dependent dehydration of t^{6}A to form ct^{6}A (9). In addition, ms^{2}t^{6}A is present in tRNA^{Lys} from *B. subtilis* (21,22). These observations strongly suggest that, in *B. subtilis*, ms^{2}t^{6}A in tRNA^{Lys} is converted to ms^{2}ct^{6}A by the TcdA homolog.

To confirm the presence of ms^{2}ct^{6}A, total RNA of *B. subtilis* was digested into nucleosides under conventional or neutral conditions, and then subjected to LC/MS analysis (Figure 2A). In the conventional conditions, we observed proton adducts of t^{6}A and ms^{2}t^{6}A, but no ct^{6}A, as reported previously (9). On the other hand, in the neutral conditions, ct^{6}A was clearly detected. In addition, we detected a dehydrated form of ms^{2}t^{6}A (m/z 441). This modified species, tentatively named N^{440}, was not detected in total nucleosides digested in the conventional conditions, indicating that it was susceptible to hydrolysis (Figure 2A). This observation strongly suggested that N^{440} is ms^{2}ct^{6}A.

Considering that *B. subtilis* tRNA^{Lys} has ms^{2}t^{6}A at position 37 (Figure 1B) (17), ms^{2}ct^{6}A should be found in this tRNA. *B. subtilis* tRNA^{Lys} was isolated by the reciprocal circulating chromatography (9,31), digested by RNase T$_1$ and subjected to capillary LC coupled to ESI/MS. The 12 mer-fragments containing anticodon region were clearly detected. Judging from the m/z values of triply-charged negative ions of this fragment (Figure 2B), we clearly detected three fragments having different modifications at position 37, namely ms^{2}A, ms^{2}t^{6}A and ms^{2}ct^{6}A. Although ms^{2}t^{6}A37 was present more abundant than ms^{2}ct^{6}A37 in the isolated tRNA^{Lys}, it is likely that a certain population of ms^{2}t^{6}A37 in this tRNA originates from ms^{2}ct^{6}A37 hydrolyzed during tRNA isolation by RCC. The 12 mer-fragment with ms^{2}ct^{6}A was further probed by collision-induced dissociation to map the modified residues (Figure 2C). By assignment of product ions in the CID spectrum, we unequivocally mapped cmnm^{5}s^{2}U at position 34 and ms^{2}ct^{6}A at position 37 (Figure 2C).

To determine the structure of N^{440}, we chemically synthesized ms^{2}ct^{6}A from ms^{2}t^{6}A (Supplementary Figure S2B). As reported in the accompanying paper (15), activation of the carboxyl group of t^{6}A by water-soluble carbodiimide (EDC), which facilitates cyclization of the side chain, predominantly generates the hydantoin isoform of ct^{6}A. Because we employed the same procedure as for ct^{6}A synthesis to cyclize the side chain of ms^{2}t^{6}A, the hydantoin isoform should be the predominant form in chemically synthesized ms^{2}ct^{6}A. Detailed spectroscopic analyses of the synthesized ms^{2}ct^{6}A using UV (Supplementary Figure S3B), IR (Supplementary Figure S4B), ^{1}H NMR (Supplementary Figure S5) and ^{13}C NMR (Supplementary Figure S6) supported the hydantoin isoform as observed for ct^{6}A in the accompanying paper (15). Especially, in the IR spectrum (Supplementary Figure S4B), two characteristic absorption bands at 1720 cm^{-1} and 1788 cm^{-1} are associated with C = O bond stretching in the hydantoin ring.

The synthetic ms^{2}ct^{6}A was mixed with total nucleosides of *B. subtilis* and subjected to LC/MS analyses using reverse-phase chromatography (Figure 3A), as well as hydrophilic interaction chromatography (Figure 3B). The synthetic ms^{2}ct^{6}A co-eluted with N^{440} as a single peak under both conditions. Next, we used CID to further probe the base-related ions (BH_2^+, m/z 309) of N^{440} and the synthetic ms^{2}ct^{6}A (Figure 3C). The product ions of these two compounds exhibited identical patterns (Figure 3D), and assigned in the chemical structures of the ms^{2}ct^{6}A base (Figure 3E). Collectively, these observations indicated that N^{440} is ms^{2}ct^{6}A.

Biogenesis of ms^{2}ct^{6}A in *B. subtilis*

The *yqeV* and *yrvM* of *B. subtilis* are homologs of *mtaB* and *tcdA*, respectively (9,22). To confirm that these genes are involved in ms^{2}ct^{6}A formation, we constructed a knockout of *yrvM* (Δ*yrvM*) and the double-deletion strain (Δ*yqeV*/Δ*yrvM*) by homologous recombination. Total RNA from wild-type *B. subtilis* (WT) and a series of knockout strains were digested into nucleosides and subjected to LC/MS analysis (Figure 4). In the Δ*yqeV* strain, both ms^{2}ct^{6}A and ms^{2}t^{6}A disappeared as expected and probably remained to be ct^{6}A and t^{6}A, respectively. In fact, the level of ct^{6}A increased slightly relative to that in the WT strain. In Δ*yrvM*, both ms^{2}ct^{6}A and ct^{6}A disappeared and remained to be ms^{2}t^{6}A and t^{6}A, respectively. Indeed, the levels of ms^{2}t^{6}A and t^{6}A clearly increased in this strain. In the case of Δ*yqeV*/Δ*yrvM*, all three derivatives (ms^{2}ct^{6}A, ct^{6}A and ms^{2}t^{6}A) disappeared, and relevant tRNAs only have t^{6}A. These observations demonstrated that *yqeV* (*mtaB*) and *yrvM* (*tcdA*) are responsible for 2-methylthiolation and cyclization of t^{6}A, respectively, resulting in the formation of ms^{2}ct^{6}A on tRNA^{Lys}.

Identification of ms^{2}ct^{6}A in plant tRNAs

According to phylogenetic analyses (9,40), homologs of *mtaB* and *tcdA* are encoded in plant genomes, indicating the presence of ms^{2}ct^{6}A in plant tRNAs. Indeed, ct^{6}A and ms^{2}t^{6}A were previously detected in Spinach (9) and *Eleusine coracana* (20), respectively. Therefore, we prepared total RNA from *Nicotiana tabacum*, *Spinacia oleracea* and *Arabidopsis thaliana*, and enzymatically digested these samples into nucleosides under acidic conditions. LC/MS analyses clearly detected ms^{2}ct^{6}A along with other t^{6}A derivatives in all three species of plant (Figure 5). Next, total nucleosides of spinach RNA were co-injected along with synthetic ms^{2}ct^{6}A by LC/MS using hydrophilic interaction chromatography (Supplementary Figure S8A), as well as reverse-phase chromatography (Supplementary Figure S8B). Plant ms^{2}ct^{6}A co-eluted with the synthetic molecule as a single peak under both conditions, demonstrating that ms^{2}ct^{6}A is present in plant tRNAs.

Presence of ms^{2}ct^{6}A in *T. brucei* tRNAs

We previously speculated that ms^{2}ct^{6}A is present in *T. brucei* tRNA^{Lys} (9). Total RNA from *T. brucei* was digested into nucleosides under neutral conditions and subjected to

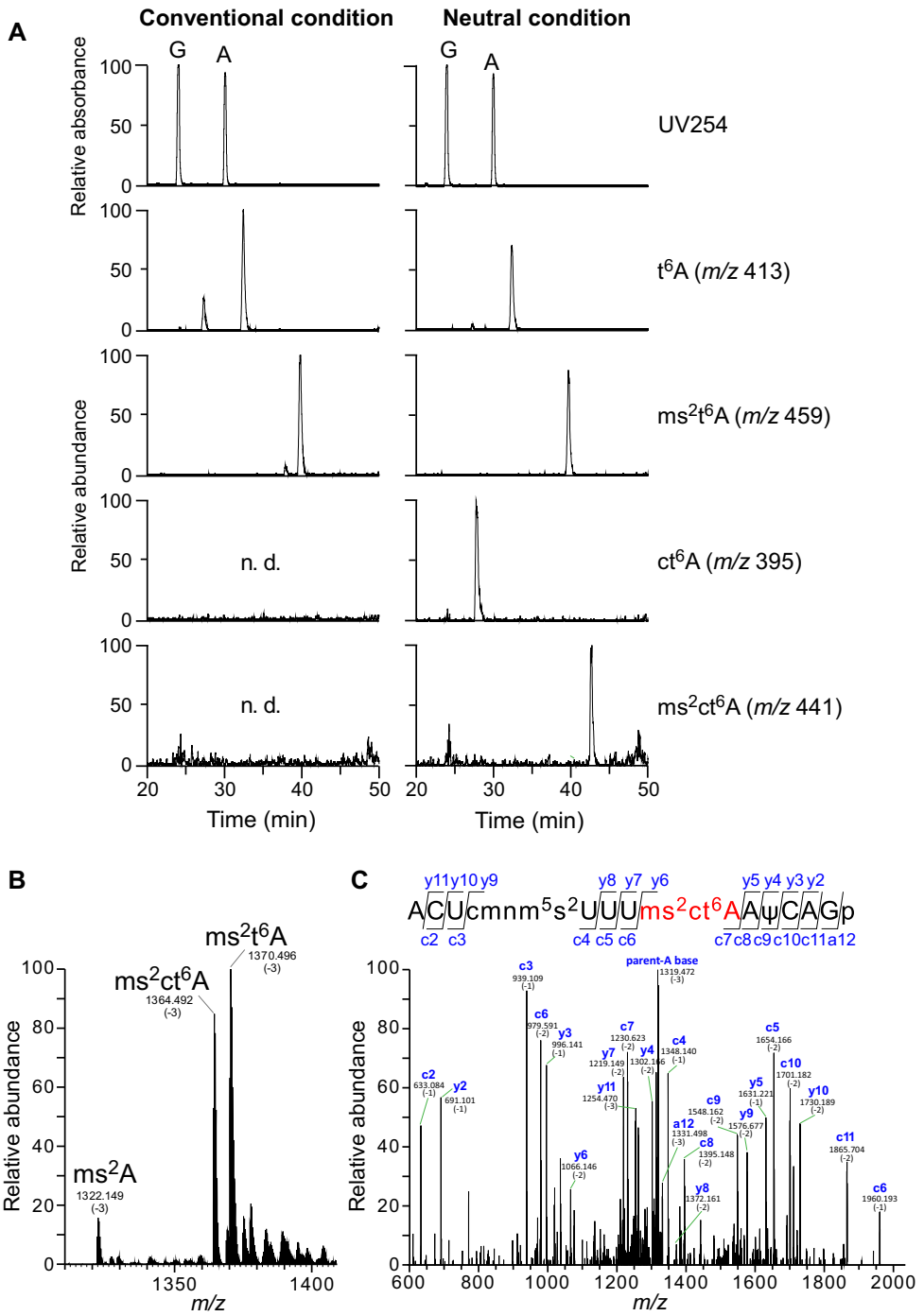

Figure 2. Mass spectrometric analyses of total RNA and isolated $tRNA^{Lys}$ from *B. subtilis*. (**A**) Nucleoside analyses of total RNA from *B. subtilis*. Total nucleosides were prepared under conventional conditions (left panels) and neutral conditions (right panels). The panels second from the bottom show mass chromatograms corresponding to the proton adducts of t^6A (*m/z* 413), ms^2t^6A (*m/z* 459), ct^6A (*m/z* 395) and ms^2ct^6A (*m/z* 441), respectively. n.d., not detected. (**B**) Mass spectrum of the 12 mer-fragments containing anticodon region. Three peaks for the triply-charged negative ions of the RNA fragments having ms^2A, ms^2t^6A and ms^2ct^6A at position 37 are indicated. (**C**) A collision-induced dissociation (CID) spectrum of the 12 mer-fragment of *B. subtilis* $tRNA^{Lys}$ digested by RNase T_1. The triply-charged negative ion of the ms^2ct^6A37-containing fragment (*m/z* 1364.492) was used as a precursor ion for CID. The product ions were assigned according to the literature (45). Sequences of parent ion and assigned product ions are described upper side in this panel.

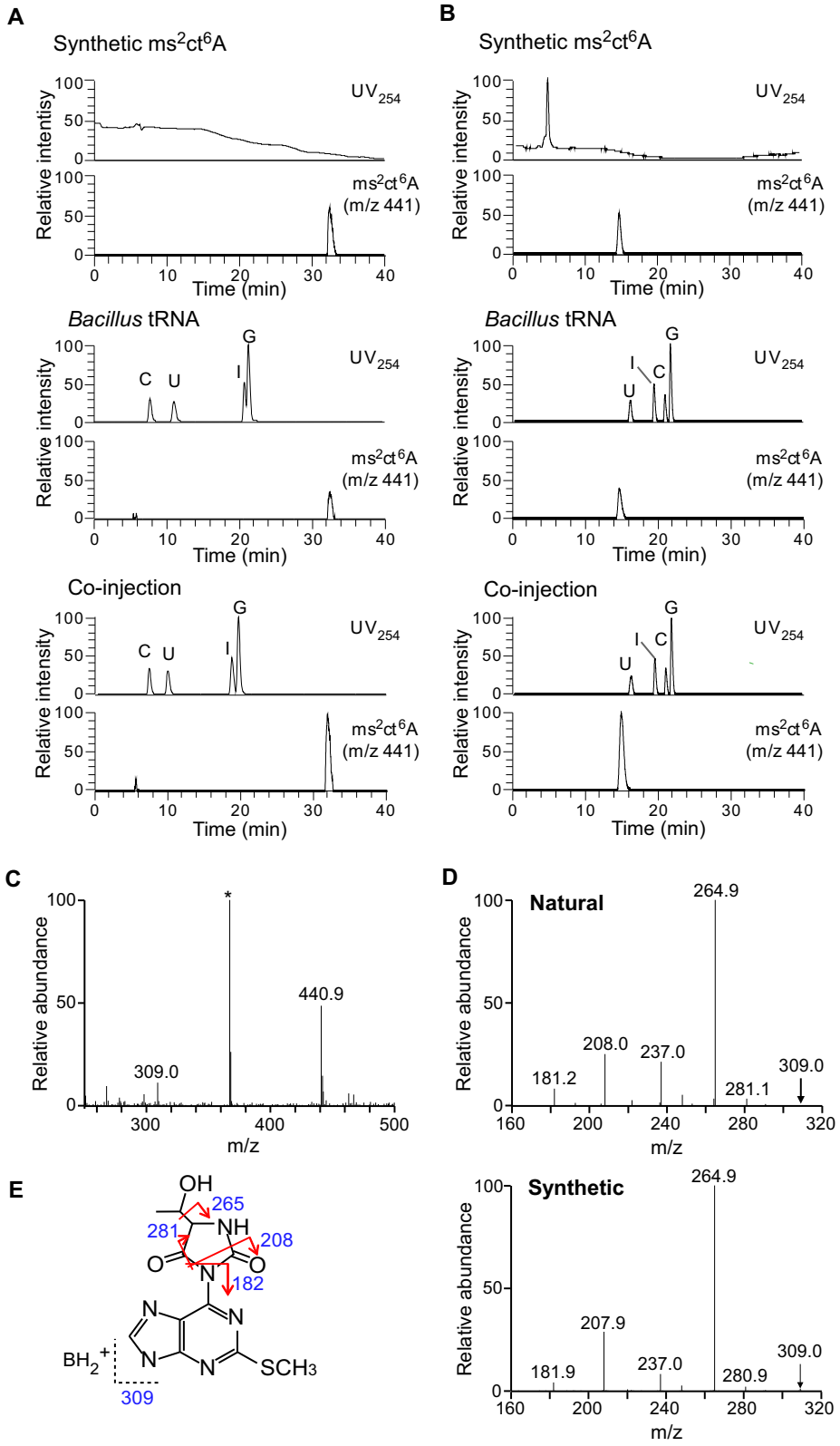

Figure 3. Structural confirmation of ms^2ct^6A from *B. subtilis*. Co-injection analyses of synthetic ms^2ct^6A and total RNA from *B. subtilis* by (**A**) RPC/ESI-MS and (**B**) HILIC/ESI-MS. UV trace at 254 nm and mass chromatograms of the synthetic ms^2ct^6A, total nucleosides of *B. subtilis* and co-injection are shown in the top, middle and bottom panels, respectively. Conversion of adenosine to inosine is due to the contamination of PDase II (Sigma P9041) with adenosine deaminase activity. (**C**) The mass spectrum for the proton adduct of natural ms^2ct^6A (MH^+, m/z 440.9) from *B. subtilis*. The base-related ion (BH_2^+, m/z 309.0) was also detected. (**D**) The CID spectra for natural (upper panel) and synthetic (lower panel) BH_2^+ of ms^2ct^6A. Parent ions for CID are indicated by arrows. (**E**) Assignment of the product ions in the CID spectrum of the natural ms^2ct^6A BH_2^+ ion.

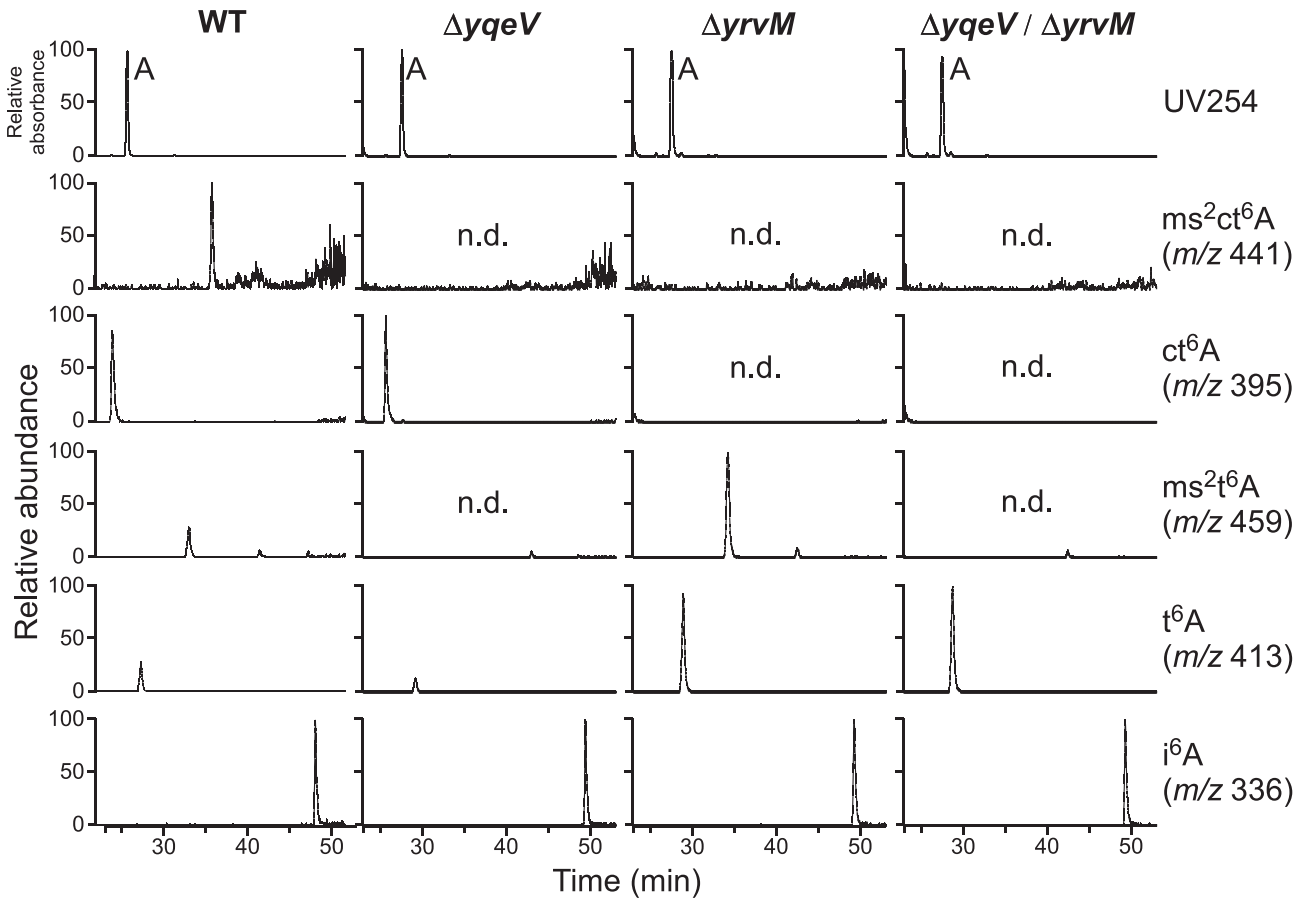

Figure 4. Identification of enzymes responsible for ms^2ct^6A formation in *B. subtilis*. RPC/ESI-MS nucleoside analyses of total RNAs from *B. subtilis* wild type (str. 168). Mass chromatograms from Δ*yqeV*, Δ*yrvM* and Δ*yqeV*/Δ*yrvM* are shown from left to right, respectively. Top panels show the UV traces at 254 nm. Panels second from the bottom show mass chromatograms corresponding to the proton adducts of ms^2ct^6A (*m/z* 441), ct^6A (*m/z* 395), ms^2t^6A (*m/z* 459), t^6A (*m/z* 413) and i^6A (*m/z* 336), respectively. n.d., not detected. Mass chromatograms of t^6A derivatives were normalized by that of i^6A, and abundance of each peak is displayed relative to the highest peak (100%) among them.

LC/MS analysis (Figure 6A). Along with ct^6A, N^{440} was clearly detectable. Next, the total nucleosides of *T. brucei* and *B. subtilis* were co-injected to LC/MS, revealing that *T. brucei* N^{440} co-eluted with *B. subtilis* ms^2ct^6A as a single peak (Figure 6B). Finally, we probed BH_2^+ of *T. brucei* N^{440} by CID (Figure 6C). The product ions exhibited a pattern identical to those of synthetic ms^2ct^6A (Figure 3D). These results demonstrated that ms^2ct^6A is also present in *T. brucei*.

Growth phenotype of *T. brucei* with hypomodified ms^2ct^6A

We hypothesized that *TbMtaB* and *TbTcdA* are responsible for the synthesis of ms^2ct^6A in *T. brucei*. To test this speculation, we generated a transgenic RNAi line for each gene and confirmed knockdown efficiency by RT-PCR. No transcript of each gene was detected in either strain, even 7 days after knockdown induced by tetracycline (Supplementary Figure S9). Upon knockdown of *TbMtaB*, ms^2ct^6A and ms^2t^6A disappeared and remained to be ct^6A and t^6A, respectively (Figure 7A). In fact, ct^6A accumulated slightly more than non-treated *T. brucei* (WT). Likewise, when *TbTcdA* was down-regulated, ms^2ct^6A and ct^6A disappeared and remained to be ms^2t^6A and t^6A, respectively (Figure 7A). To determine the physiological importance of this modification, we measured the growth rates of these strains after induction of RNAi (Figure 7B). Down-regulation of expression of either gene alone did not cause a major growth defect (data not shown). However, in the presence of non-inhibitory concentrations of cycloheximide (Chx), growth of cells with down-regulated *TbTcdA* was slowed (Figure 7B), whereas little growth phenotype was observed when *TbMtaB* was knocked down. Thus, hypomodification of ms^2ct^6A and ct^6A results in sensitivity to an antibiotic that targets the ribosome, suggesting that cyclization of these modifications contributes to efficient cell growth and protein synthesis.

DISCUSSION

Because ct^6A is a chemically labile derivative of t^6A, it had never been detected by conventional nucleoside analysis for more than 40 years since t^6A's discovery. ct^6A can be detected only if total RNA is extracted from the cell under acidic conditions and digested into nucleosides under neutral conditions, explaining why ms^2ct^6A has not been detected previously. In this study, we performed nucleoside analysis under neutral or acidic conditions and successfully

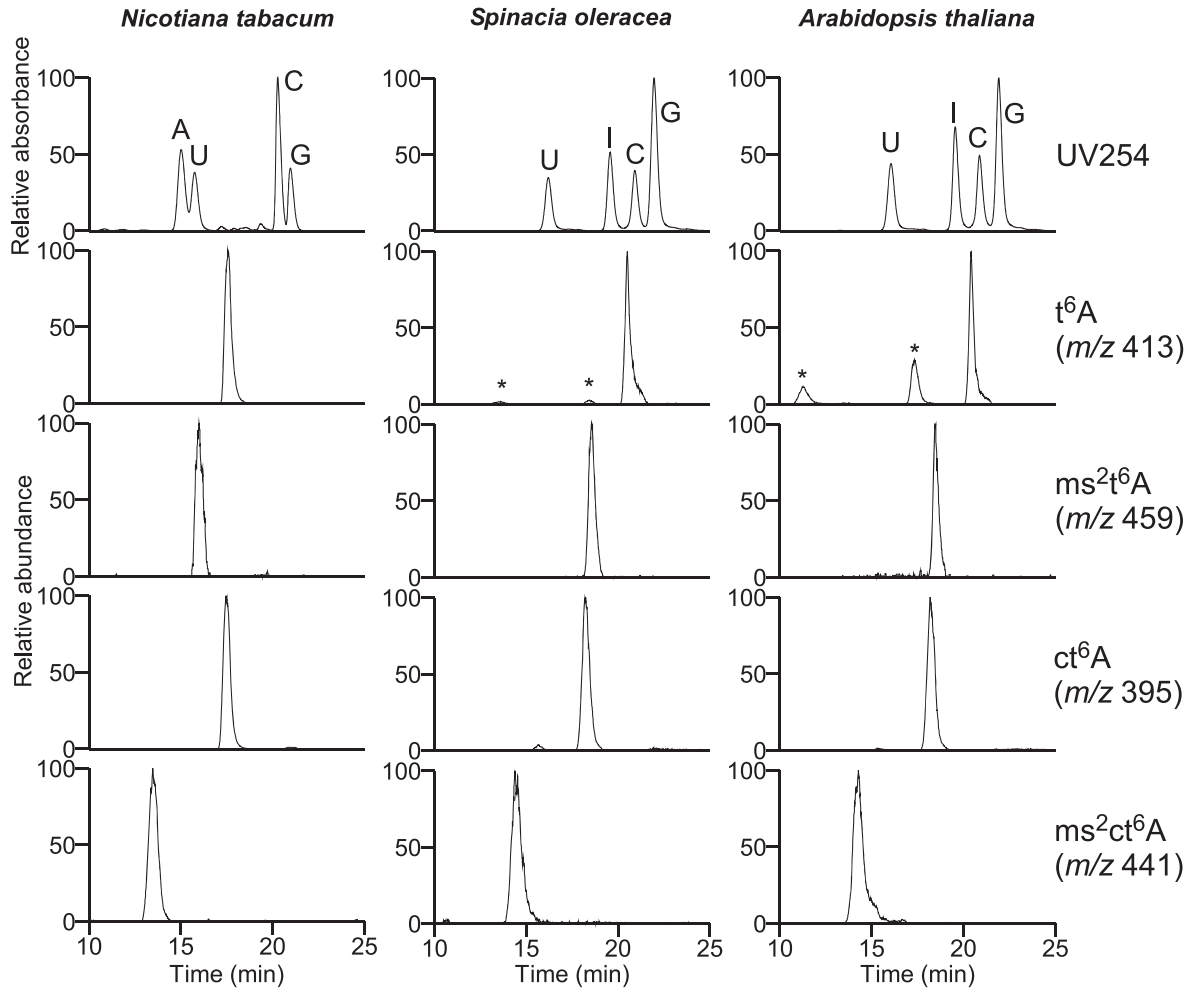

Figure 5. Detection of ms^2ct^6A in plant tRNAs. HILIC/ESI-MS nucleoside analyses of total RNAs from *N. tabacum*, *S. oleracea* and *A. thaliana*. Top panels show UV traces at 254 nm. Panels second from the bottom show mass chromatograms corresponding to the proton adducts of t^6A (m/z 413), ms^2t^6A (m/z 459), ct^6A (m/z 359) and ms^2ct^6A (m/z 441), respectively. Unassigned peaks are indicated by asterisks. Conversion of adenosine to inosine observed in spinach and *A. thaliana* is due to the contamination of adenosine deaminase activity in PDase II (Sigma P9041).

identified ms^2ct^6A in total RNA samples from *B. subtilis*, three plants and *T. brucei*. Because we also detected t^6A and ms^2t^6A, we assume that ct^6A and ms^2ct^6A are partial modifications in these organisms, indicating that cyclization of t^6A and ms^2t^6A might be regulated under certain physiological conditions.

By referring to the synthetic nucleoside as a reference, the chemical structure of ms^2ct^6A was determined to be a hydantoin isoform, rather than an oxazolone isoform previously predicted. According to the structural analysis of ct^6A nucleoside (15), two carbonyl oxygen atoms of the hydantoin ring are repulsive to the nitrogen atoms (N1 and N7) of the adenine base (Supplementary Figure S1). Consistent with this, the C6-N6 bond length is longer than the normal C-N bond length. Therefore, the hydantoin ring adopts a twisted position against the adenine base with a torsion angle of -52.7°. In light of this observation, it is difficult to speculate how the hydantoin ring of ct^6A contributes to the efficient decoding of tRNA on the ribosome. Structural studies of ribosomes in complex with tRNA containing ct^6A or ms^2ct^6A will be necessary to reveal the functional and structural roles of these modifications in protein synthesis.

We now know of five species of t^6A derivatives (Figure 1A and S1), of which ms^2ct^6A is the most chemically complex. Initially, t^6A is formed at position 37 on tRNAs with NNU anticodons (i.e. those responsible for ANN codons) (Figure 8). This process is catalyzed by multiple enzymes (TsaB, TsaC, TsaD and TsaE in bacteria) using L-threonine, bicarbonate and ATP as substrates. In $tRNA^{Thr}$ from certain species of γ-proteobacteria, m^6t^6A37 is formed via the methylation of t^6A37 by TrmO using AdoMet as a substrate. In some species of bacteria, fungi, plants and protists, ct^6A37 is formed via the cyclization of t^6A37 by ATP-dependent dehydration by TcdA. In organisms that harbor an MtaB homolog, t^6A37 and ct^6A37 are 2-thiomethylated to form ms^2t^6A and ms^2ct^6A, respectively. According to the nucleoside analyses of *B. subtilis* knockout strains, 2-methylthiolation and cyclization of t^6A are independent reactions involved in synthesis of ms^2ct^6A (Figure 8).

In terms of phylogenetic distribution, ms^2ct^6A should be present in organisms with MtaB and TcdA orthologs.

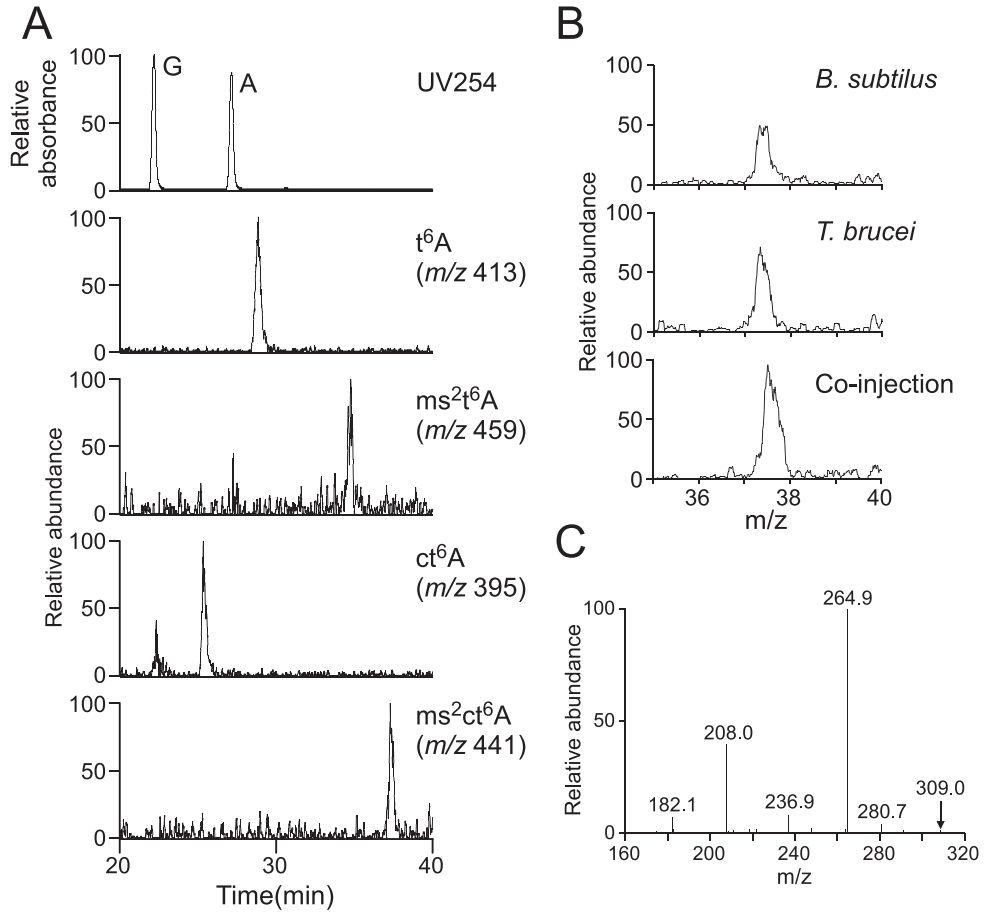

Figure 6. Detection of ms^2ct^6A in *T. brucei* tRNAs. (**A**) RPC/ESI-MS nucleoside analyses of total RNAs from *T. brucei*. Top panel shows a UV trace at 254 nm. Panels second from the bottom show mass chromatograms corresponding to the proton adducts of t^6A (*m/z* 413), ms^2t^6A (*m/z* 459), ct^6A (*m/z* 395) and ms^2ct^6A (*m/z* 441), respectively. (**B**) Mass chromatograms showing the proton adduct of ms^2ct^6A (*m/z* 441) in total nucleosides of *B. subtilis* (top panel), *T. brucei* (middle panel) and the co-injection fraction (bottom panel) obtained by RPC/ESI-MS. (**C**) CID spectrum of BH_2^+ of ms^2ct^6A from *T. brucei*. The parent ion for CID is indicated by an arrow.

Among bacteria, δ-proteobacteria and approximately half of the species that compose Firmicutes and Bacteroidetes encode these two enzymes in their genomes. In protists, ms^2ct^6A is found in *Trypanosoma* and *Tetrahymena*. In Archaeplastida, both MtaB and TcdA are present in Plants and Chlorophyta, but not in Rhodophyta or Glaucophyta.

In *E. coli*, ct^6A37 is involved in the decoding activity of $tRNA^{Lys}$ (9). *tcdA* engages in a genetic interaction with *mnmA*, as demonstrated by the observation that a synthetic growth reduction occurs when both genes are deleted simultaneously. Considering that *mnmA* encodes a 2-thiouridylase to form mnm^5s^2U at the wobble position of $tRNA^{Lys}$, which also contains ct^6A37, cyclization of ct^6A37 must play a functional role in the decoding activity of $tRNA^{Lys}$.

The functional role of the 2-methylthio modification was first studied in an *in vitro E. coli* translation system using tRNA containing ms^2i^6A37. *E. coli* $tRNA^{Phe}$ containing the ms^2-modification was more active in poly(U)-dependent poly(Phe) synthesis than tRNA lacking the ms^2-modification (41). In *Salmonella typhimurium*, +1 frameshift activities of $tRNA^{Phe}$ and $tRNA^{Tyr}$ at the ribosomal P-site were significantly higher when they lacked the ms^2-modification (42), indicating that 2-methylthiolation of ms^2i^6A37 plays a critical role in maintaining the reading frame during elongation. The structure of ms^2i^6A37 in tRNA has revealed that the 2-methylthio group stabilizes the codon–anticodon interaction through cross-strand stacking with the first base of the P-site codon (43). This stabilization effect might contribute to the prevention of +1 frameshifting.

In the case of ms^2t^6A modification in *B. subtilis*, the decoding ability of $tRNA^{Lys}$ with or without the ms^2-modification was examined using a luciferase reporter. The results showed that the ms^2-modification is required to decode AAA and AAG codons efficiently (23). Given that a large fraction of ms^2t^6A37 must be converted to ms^2ct^6A37 in *B. subtilis* $tRNA^{Lys}$, this finding throws light on the function of the ms^2-modification of ms^2ct^6A37 (but not of ms^2t^6A37). However, no significant growth or temperature-sensitivity phenotypes have been observed to date in *ΔyqeV*, *ΔyrvM* or the double-deletion strains (data not shown). Future studies should investigate whether phenotypes emerge under various stress or culture conditions. In *T. brucei*, we observed a growth delay after knockdown of *TbTcdA* in the presence of non-inhibitory concentration

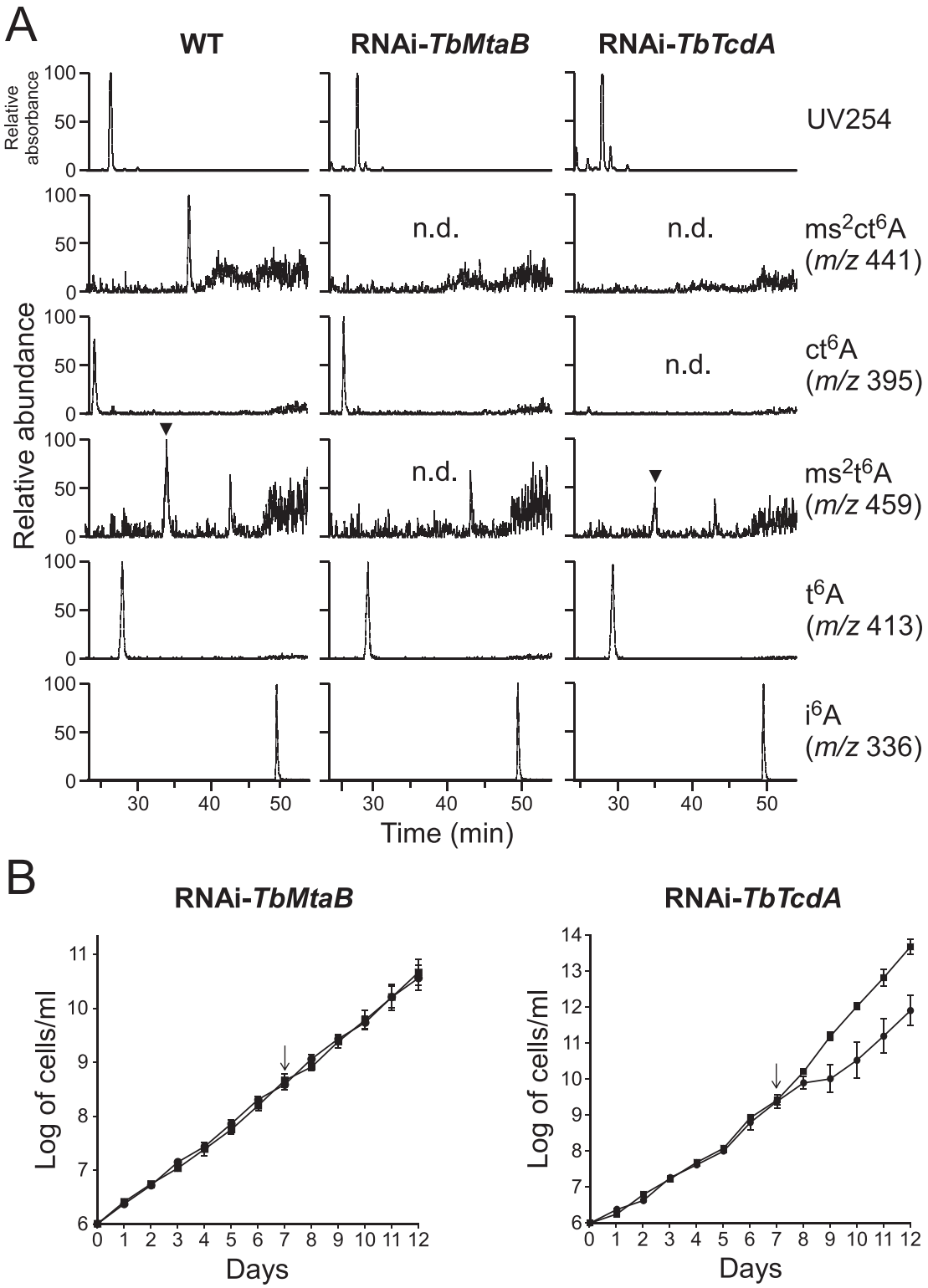

Figure 7. Biogenesis of ms^2ct^6A and growth phenotype of *T. brucei* with hypomodified tRNAs. (**A**) RPC/ESI-MS nucleoside analyses of total RNAs from *T. brucei* wild type (left panels) and transgenic RNAi lines of *TbMtaB* (middle panels) and *TbTcdA* (right panels). Mass chromatograms of t^6A derivatives were normalized by that of i^6A, and abundance of each peak is displayed relative to the highest peak (100%) among them. Top panels show the UV traces at 254 nm. Panels second from the bottom show mass chromatograms detecting the proton adducts of ms^2ct^6A (*m/z* 441), ct^6A (*m/z* 395), ms^2t^6A (*m/z* 459), t^6A (*m/z* 413) and i^6A (*m/z* 336), respectively. n.d., not detected. (**B**) Growth curves of *T. brucei* transgenic RNAi lines of *TbMtaB* (left) and *TbTcdA* (right). Cumulative cell counts indicated by logarithmic cell number (Log of cells/ml) were measured in the presence of non-inhibitory concentration of cycloheximide. RNAi was induced by adding (black circle) or not adding (black square) tetracycline (Tet) at 7 days (as indicated by arrow) after inoculation.

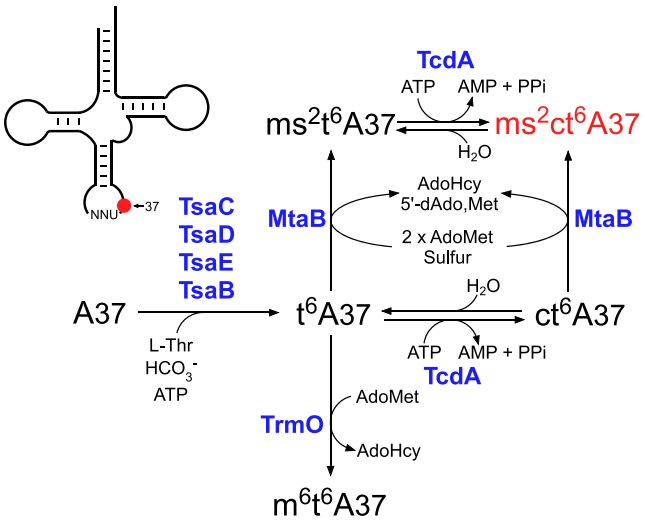

Figure 8. Biosynthetic pathway of ms^2ct^6A and other t^6A derivatives. In bacteria, A37 of tRNAs responsible for ANN codons is modified to t^6A by multiple enzymes (TsaB, TsaC, TsaD and TsaE) using L-threonine, bicarbonate and ATP as substrates. In $tRNA^{Thr}$ from γ-proteobacteria, t^6A37 is methylated by TrmO using AdoMet to form m^6t^6A37. In certain populations of bacteria, fungi, plant and protists, t^6A37 is cyclized by TcdA using ATP to form ct^6A37. In organisms bearing an MtaB homolog, t^6A37 and ct^6A37 in particular tRNAs are 2-thiomethylated by MtaB to form ms^2t^6A37 and ms^2ct^6A37, respectively.

of cycloheximide, indicating defective decoding activity of $tRNA^{Lys}$ with hypomodified ms^2ct^6A. To obtain a deeper understanding of the physiological role of this modification, future studies should be directed toward analyzing the phenotypic features of *T. brucei* knockdown lines.

SUPPLEMENTARY DATA

Supplementary Data are available at NAR Online.

ACKNOWLEDGEMENTS

The authors are grateful to the members of the Suzuki laboratory, in particular Takaaki Taniguchi for technical support and many insightful discussions.

FUNDING

National Science Centre in Poland [UMO-2014/13/N/ST5/01591 to M.M.]; National Institute of General Medical Sciences of the National Institues of Health [R01GM084065 to J.D.A.]; Ministry of Education, Culture, Sports, Science and Technology of Japan (MEXT) [to T.S.]; Japan Society for the Promotion of Science (JSPS) [to T.S.]. Funding for open access charge: Grants-in-Aid for Scientific Research on Priority Areas from the Ministry of Education, Science, Sports and Culture of Japan.
Conflict of interest statement. None declared.

REFERENCES

1. Frye,M., Jaffrey,S.R., Pan,T., Rechavi,G. and Suzuki,T. (2016) RNA modifications: what have we learned and where are we headed? *Nat. Rev. Genet.*, **17**, 365–372.
2. Machnicka,M.A., Milanowska,K., Osman Oglou,O., Purta,E., Kurkowska,M., Olchowik,A., Januszewski,W., Kalinowski,S., Dunin-Horkawicz,S., Rother,K.M. *et al.* (2013) MODOMICS: a database of RNA modification pathways–2013 update. *Nucleic Acids Res.*, **41**, D262–D267.
3. Grosjean,H. (2009) DNA and RNA Modification Enzymes: Structure, Mechanism, Function and Evolution. In: Grosjean,H (ed). *Molecular Biology Intelligence Unit*. Landes Bioscience, Austin, pp. 1–18.
4. Yokoyama,S. and Nishimura,S. (1995) Modified nucleosides and codon recognition. In: Soll,DR and RajBhandary,U (eds). *tRNA: Structure, Biosynthesis, and Function*. American Society for Microbiology, Washington, D.C., pp. 207–223.
5. Bjork,G. (1995) Biosynthesis and function of modified nucleosides. In: Soll,DR and RahBhandary,U (eds). *tRNA: Structure, Biosynthesis, and Function*. American Society for Microbiology, Washington, D.C., pp. 165–205.
6. Suzuki,T. (2005) In: Biosynthesis and function of tRNA wobble modifications. In: Grosjean,H (ed). *Fine-Tuning of RNA Functions by Modification and Editing*. Springer-Verlag Berlin and Heidelberg GmbH & Co. KG, Berlin Heidelberg, Vol. **12**, pp. 23–69.
7. Bjork,G.R. and Hagervall,T.G. (2014) Transfer RNA modification: presence, synthesisand function. *EcoSal Plus*, doi:10.1128/ecosalplus.ESP-0007-2013.
8. Thiaville,P.C., Iwata-Reuyl,D. and de Crecy-Lagard,V. (2014) Diversity of the biosynthesis pathway for threonylcarbamoyladenosine (t(6)A), a universal modification of tRNA. *RNA Biol.*, **11**, 1529–1539.
9. Miyauchi,K., Kimura,S. and Suzuki,T. (2013) A cyclic form of N6-threonylcarbamoyladenosine as a widely distributed tRNA hypermodification. *Nat. Chem. Biol.*, **9**, 105–111.
10. Srinivasan,M., Mehta,P., Yu,Y., Prugar,E., Koonin,E.V., Karzai,A.W. and Sternglanz,R. (2011) The highly conserved KEOPS/EKC complex is essential for a universal tRNA modification, t6A. *EMBO J.*, **30**, 873–881.
11. El Yacoubi,B., Hatin,I., Deutsch,C., Kahveci,T., Rousset,J.P., Iwata-Reuyl,D., Murzin,A.G. and de Crecy-Lagard,V. (2011) A role for the universal Kae1/Qri7/YgjD (COG0533) family in tRNA modification. *EMBO J.*, **30**, 882–893.
12. Perrochia,L., Guetta,D., Hecker,A., Forterre,P. and Basta,T. (2013) Functional assignment of KEOPS/EKC complex subunits in the biosynthesis of the universal t6A tRNA modification. *Nucleic Acids Res.*, **41**, 9484–9499.
13. Schweizer,M.P., Chheda,G.B., Baczynskyj,L. and Hall,R.H. (1969) Aminoacyl nucleosides. VII. N-(Purin-6-ylcarbamoyl)threonine. A new component of transfer ribonucleic acid. *Biochemistry*, **8**, 3283–3289.
14. Matuszewski,M. and Sochacka,E. (2014) Stability studies on the newly discovered cyclic form of tRNA N(6)-threonylcarbamoyladenosine (ct(6)A). *Bioorg. Med. Chem. Lett.*, **24**, 2703–2706.
15. Matuszewski,M., Wojciechowski,J., Miyauchi,K., Gdaniec,Z., Wolf,W.M., Suzuki,T. and Sochacka,E. (2016) A hydantoin isoform of cyclic N^6-threonylcarbamoyladenosine (ct^6A) is present in tRNAs. *Nucleic Acids Res.*, doi:10.1093/nar/gkw1189.
16. Kimura,S., Miyauchi,K., Ikeuchi,Y., Thiaville,P.C., Crecy-Lagard,V. and Suzuki,T. (2014) Discovery of the beta-barrel-type RNA methyltransferase responsible for N6-methylation of N6-threonylcarbamoyladenosine in tRNAs. *Nucleic Acids Res.*, **42**, 9350–9365.
17. Yamada,Y. and Ishikura,H. (1981) The presence of *N*-[(9-*b*-D-ribofuranosyl-2-methylthiopurin-6-yl)carbamoyl]threonine in lysine tRNA1 from *Bacillus subtilis*. *J. Biochem.*, **89**, 1589–1591.
18. Yamaizumi,Z., Nishimura,S., Limburg,K., Raba,M., Gross,H.J., Crain,P.F. and McCloskey,J.A. (1979) Structure elucidation by high-resolution mass-spectrometry of a highly modified nucleoside from mammalian transfer-Rna - *N*-[(9-*b*-D-Ribofuranosyl-2-Methylthiopurin-6-yl)Carbamoyl]threonine. *J. Am. Chem. Soc.*, **101**, 2224–2225.
19. Krog,J.S., Espanol,Y., Giessing,A.M., Dziergowska,A., Malkiewicz,A., de Pouplana,L.R. and Kirpekar,F. (2011) 3-(3-amino-3-carboxypropyl)-5,6-dihydrouridine is one of two novel post-transcriptional modifications in tRNALys(UUU) from Trypanosoma brucei. *FEBS J.*, **278**, 4782–4796.

20. Raviprakash,K.S. and Cherayil,J.D. (1984) Multiple species of thionucleosides in ragi (Eleusine coracana) tRNA. *Curr. Sci.*, **53**, 847–851.
21. Anton,B.P., Russell,S.P., Vertrees,J., Kasif,S., Raleigh,E.A., Limbach,P.A. and Roberts,R.J. (2010) Functional characterization of the YmcB and YqeV tRNA methylthiotransferases of *Bacillus subtilis*. *Nucleic Acids Res.*, **38**, 6195–6205.
22. Arragain,S., Handelman,S.K., Forouhar,F., Wei,F.Y., Tomizawa,K., Hunt,J.F., Douki,T., Fontecave,M., Mulliez,E. and Atta,M. (2010) Identification of eukaryotic and prokaryotic methylthiotransferase for biosynthesis of 2-methylthio-N^6-threonylcarbamoyladenosine in tRNA. *J. Biol. Chem.*, **285**, 28425–28433.
23. Wei,F.Y., Suzuki,T., Watanabe,S., Kimura,S., Kaitsuka,T., Fujimura,A., Matsui,H., Atta,M., Michiue,H., Fontecave,M. *et al.* (2011) Deficit of tRNA(Lys) modification by Cdkal1 causes the development of type 2 diabetes in mice. *J. Clin. Invest.*, **121**, 3598–3608.
24. Wei,F.Y. and Tomizawa,K. (2011) Functional loss of Cdkal1, a novel tRNA modification enzyme, causes the development of type 2 diabetes. *Endocr. J.*, **58**, 819–825.
25. Kasai,H., Murao,K., Nishimura,S., Liehr,J.G., Crain,P.F. and Mccloskey,J.A. (1976) Structure determination of a modified nucleoside isolated from Escherichia-coli transfer Ribonucleic-acid - N-[N-[(9-Beta-D-Ribofuranosylpurin-6-Yl)Carbamoyl]Threonyl]2-Amido-2-Hydroxymethylpropane-1,3-Diol. *Eur. J. Biochem.*, **69**, 435–444.
26. Vagner,V., Dervyn,E. and Ehrlich,S.D. (1998) A vector for systematic gene inactivation in Bacillus subtilis. *Microbiology*, **144**, 3097–3104.
27. Kobayashi,K. (2007) Bacillus subtilis pellicle formation proceeds through genetically defined morphological changes. *J. Bacteriol.*, **189**, 4920–4931.
28. Kobayashi,K., Shoji,K., Shimizu,T., Nakano,K., Sato,T. and Kobayashi,Y. (1995) Analysis of a suppressor mutation ssb (kinC) of sur0B20 (spo0A) mutation in Bacillus subtilis reveals that kinC encodes a histidine protein kinase. *J. Bacteriol.*, **177**, 176–182.
29. Kumagai-Sano,F., Hayashi,T., Sano,T. and Hasezawa,S. (2006) Cell cycle synchronization of tobacco BY-2 cells. *Nat. Protoc.*, **1**, 2621–2627.
30. Yoshida,M., Kataoka,N., Miyauchi,K., Ohe,K., Iida,K., Yoshida,S., Nojima,T., Okuno,Y., Onogi,H., Usui,T. *et al.* (2015) Rectifier of aberrant mRNA splicing recovers tRNA modification in familial dysautonomia. *Proc. Natl. Acad. Sci. U.S.A.*, **112**, 2764–2769.
31. Miyauchi,K., Ohara,T. and Suzuki,T. (2007) Automated parallel isolation of multiple species of non-coding RNAs by the reciprocal circulating chromatography method. *Nucleic Acids Res.*, **35**, e24.
32. Crain,P.F. (1990) Preparation and enzymatic hydrolysis of DNA and RNA for mass spectrometry. *Methods Enzymol.*, **193**, 782–790.
33. Sakaguchi,Y., Miyauchi,K., Kang,B.I. and Suzuki,T. (2015) Nucleoside analysis by hydrophilic interaction liquid chromatography coupled with mass spectrometry. *Methods Enzymol.*, **560**, 19–28.
34. Suzuki,T., Ikeuchi,Y., Noma,A., Suzuki,T. and Sakaguchi,Y. (2007) Mass spectrometric identification and characterization of RNA-modifying enzymes. *Methods Enzymol.*, **425**, 211–229.
35. Chheda,G. and Hong,C.I. (1971) Synthesis of naturally occurring 6-ureidopurines and their nucleosides. *J. Med. Chem.*, **14**, 748–753.
36. Davis,D.R. and Bajji,A.C. (2005) Introduction of hypermodified nucleotides in RNA. *Methods Mol. Biol.*, **288**, 187–204.
37. Hong,C.I. and Chheda,G.B. (1972) N-[(9-β-D-ribofuranosyl-9H-purin-6-yl)carbamoyl]-L-threonine (t6A). Synthesis via ethyl 9- β-D-ribofuranosylpurine-6-carbamate. In: Towsend,LB and Tipson,RS (eds). *Nucleic Acid Chemistry*. John Wiley & Sons, NY, pp. 661–664.
38. Kierzek,E. and Kierzek,R. (2003) The synthesis of oligoribonucleotides containing N6-alkyladenosines and 2-methylthio-N6-alkyladenosines via post-synthetic modification of precursor oligomers. *Nucleic Acids Res.*, **31**, 4461–4471.
39. Chomczynski,P. and Sacchi,N. (1987) Single-step method of RNA isolation by acid guanidinium thiocyanate-phenol-chloroform extraction. *Anal. Biochem.*, **162**, 156–159.
40. Kaminska,K.H., Baraniak,U., Boniecki,M., Nowaczyk,K., Czerwoniec,A. and Bujnicki,J.M. (2008) Structural bioinformatics analysis of enzymes involved in the biosynthesis pathway of the hypermodified nucleoside ms(2)io(6)A37 in tRNA. *Proteins*, **70**, 1–18.
41. Buck,M. and Griffiths,E. (1982) Iron mediated methylthiolation of tRNA as a regulator of operon expression in Escherichia coli. *Nucleic Acids Res.*, **10**, 2609–2624.
42. Urbonavicius,J., Qian,Q., Durand,J.M., Hagervall,T.G. and Bjork,G.R. (2001) Improvement of reading frame maintenance is a common function for several tRNA modifications. *EMBO J.*, **20**, 4863–4873.
43. Jenner,L.B., Demeshkina,N., Yusupova,G. and Yusupov,M. (2010) Structural aspects of messenger RNA reading frame maintenance by the ribosome. *Nat. Struct. Mol. Biol.*, **17**, 555–560.
44. Sprinzl,M. and Vassilenko,K.S. (2005) Compilation of tRNA sequences and sequences of tRNA genes. *Nucleic Acids Res.*, **33**, D139–D140.
45. McLuckey,S.A., Van Berkel,G.J. and Glish,G.L. (1992) Tandem mass spectrometry of small, multiply charged oligonucleotides. *J. Am. Soc. Mass Spectrom.*, **3**, 60–70.